Fusion Technology

ISSN: 0748-1896 (Print) (Online) Journal homepage: http://www.tandfonline.com/loi/ufst19

Calorimetric Experiments Supporting the Transmission Resonance Model for Cold Fusion

Robert D. Eagleton & Robert T. Bush

To cite this article: Robert D. Eagleton & Robert T. Bush (1991) Calorimetric Experiments Supporting the Transmission Resonance Model for Cold Fusion, Fusion Technology, 20:2, 239-245, DOI: 10.13182/FST91-A29695

To link to this article: http://dx.doi.org/10.13182/FST91-A29695

CALORIMETRIC EXPERIMENTS SUPPORTING THE TRANSMISSION RESONANCE MODEL FOR COLD FUSION

COLD FUSION

TECHNICAL NOTE

KEYWORDS: *cold fusion, calorimetry, transmission resonance model*

ROBERT D. EAGLETON and ROBERT T. BUSH
California State Polytechnic University, Physics Department
3801 West Temple Avenue, Pomona, California 91768

Received January 11, 1991
Accepted for Publication April 30, 1991

The experimental details of calorimetric experiments that provide support for the transmission resonance model (TRM) to explain cold fusion are presented. For the first time, a theoretical model provides a good fit to calorimetric data and permits an understanding of that data. After the first experiment in which excess power was achieved, the model was employed to guide further experiments. Not only does the TRM suggest which experimental parameters to hold fixed and which to vary, it also predicts significant nonlinear structure and guides the search for that structure. The following are described: calorimeter and cell designs, electrode preparation, electrode charging, and excess power measurements.

INTRODUCTION

As described in Ref. 1, the transmission resonance model (TRM) predicts that the excess power produced by an electrolytic cold fusion cell should vary in a rather unique manner as the applied current density i and the cell temperature T are varied. To test this hypothesis, two experiments were conducted: (a) Excess power was measured as a function of i while T was held constant, and (b) excess power was measured as a function of cell temperature T while i was held fixed.

The experiments employed a modified Fleischmann-Pons[2] electrolytic cell. There were, however, three principal modifications: (a) the use of a *platinum recombiner* near the top of the cell that allowed for *closed-cell operation*, (b) a *magnetic stirrer* that provided for more uniform mixing of the electrolyte, and (c) the use of *Teflon* to protect all nonelectrode metal surfaces from exposure to the electrolyte.

Of the six cells, excess power was recorded for two, cells 4 and 5. Cell 1, the original cell, was run as a blank with regular (light) water rather than heavy water. Its open calorimeter design was so rudimentary that the bath temperature could not be controlled. Cell 2 was run with heavy water but employed the same rudimentary open calorimeter that was used with cell 1. Cell 3 employed heavy water and an upgraded design, shown in Fig. 1. It was run simultaneously with cell 4 under what were thought to be essentially identical conditions. However, a postcharacterization indicated that the cell 3 electrolyte was covered with a film of silicone oil. This silicone oil film most likely originated in the "bubbler" shown in Fig. 1. This may well have caused the difference in behavior between cells 3 and 4. Cell 6 is currently a bit of a mystery. It was intended to be run as a twin of cell 5, which did give excess power. However, cell 6 did not give excess power, and it is not clear why it did not. Note, however, that the TRM suggests that cold fusion may well be a chaotic phenomenon. If this is true, it would be possible to load two identical cathodes under identical conditions and find them behaving quite differently 10 days after the beginning of loading.

EXPERIMENTAL DETAILS

The electrolytic cells were positioned within forced-flow calorimeters as shown in Fig. 1. The calorimeter consisted of a water bath surrounded by 1 in. of Styrofoam. The temperature of the bath was controlled by regulating the temperature of the coolant (water), which flowed through a copper coil immersed within the bath. Six Fluke 80PK-1 type K thermocouples were used to monitor the cell, bath, and coolant temperatures. In addition to manual data logging, an Apple IIe-compatible data acquisition system, Analog Connection II, was used to record the temperatures at 12-min intervals. The thermocouples were located as follows: one at the coolant inlet port, one at the coolant outlet port, two within the bath between the coolant coil and the outer cell wall, and two within the electrolytic cell.

The closed-cell configuration is shown in Fig. 1. It was constructed of polypropylene and capped with a rubber stopper. A recombiner in the form of platinum metal powder attached to a nickel substrate located in the air cavity at the top of the cell was used to recombine the oxygen and deuterium gas within the cell. The electrolyte consisted of a 0.1 M solution of LiOD in 99.9% D_2O. Platinum-clad niobium wire in the form of a 1.5-cm-diam helical coil was used for the anode with the palladium cathode located along its axis. The 0.25- × 1- × 2-cm cathode was cut from an Engelhard 99.9% palladium investment bar and welded to a 99.9% silver wire.

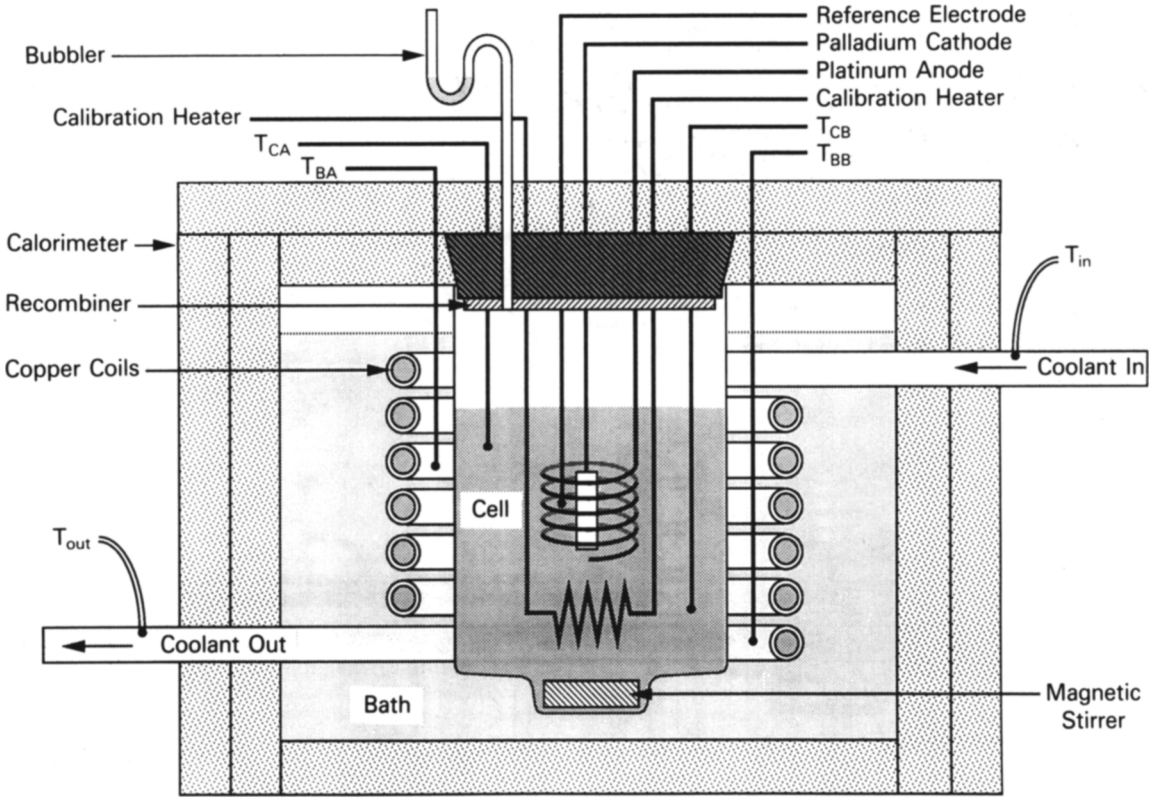

Fig. 1. Schematic of calorimeter and electrolytic cell.

A Nichrome heating element enclosed in a Teflon sleeve was used for cell calibration. Teflon sleeves enclosed the silver electrode lead and thermocouples to reduce electrolyte contamination. Uniform heating of the electrolyte was ensured by the use of a Teflon-coated magnetic stirrer.

PRETREATMENT AND CHARGING

Each of the electrodes had a surface area of ~4 cm^2. Pretreatment and charging were as follows: For cell 4, the cathode was washed in aqua regia for 5 min and rinsed in deionized water. It was then heat treated in air at 200°C for 24 h. Charging was carried out at 30 mA/cm^2 for 6 days before testing for excess power. For cell 5, the cathode was cold worked via compression in a vise. Annealing was begun in air at 600°C for 8 h, followed by 350°C in air for 16 h and 650°C in nitrogen gas for 1 h. Charging took place for 19 days at 60 mA/cm^2 before testing for excess power.

EXPERIMENTAL PROCEDURES

Cell Calibration

The cells were calibrated by determining the steady-state temperature difference across the cell walls as a function of electrical power supplied to the Nichrome heater. Two calibration curves were obtained per cell by taking the difference between the average electrolyte temperature and each of the two bath temperature measurements T_{BA} and T_{BB} of Fig. 1. The calibration curve for cell 4 is shown in Fig. 2.

Excess Power Measurements

A palladium electrode was monitored for excess power production by comparing the electrical power input and the steady-state temperature difference for its electrolytic cell with those of the calibration curve for that cell. These data points are identified by the symbols associated with the "check for excess power" in Fig. 2. Excess power was computed by subtracting the electrical power delivered to the cell from the calibrated power required for a measured temperature difference. The major error in the excess power measurement was due to a ±0.2°C uncertainty in the temperature measurements. Since the average slope of the power versus temperature difference curve is 1.5 W/°C, this translates into an excess power error of ±0.3 W, which is ~10% of the excess power measurements. The fact that the recombiner is not in operation during the calibration with the Nichrome heater introduces some error. However, since the recombiner is located near the top of the cell, heat tends to be conducted out of the top of the cell. Thus, if corrections for this heat loss were made, the result would be an even greater value for the total excess heat produced. Plots of electrical power input and excess power produced as a function of time for cells 4 and 5 are shown in Figs. 3 and 4, respectively. The total electrical energy delivered to cell 4 from the beginning of charging until the termination of excess power was ~2.0 MJ, while that for cell 5 was ~2.3 MJ. The respective excess heats, i.e., the time-integrated excess powers, were 0.35 and 0.2 MJ for cells 4 and 5, respectively. Tables I and II list the data associated with the excess power data points taken for cells 4 and 5, respectively. Table III summarizes pertinent information on excess heat production for the two cells.

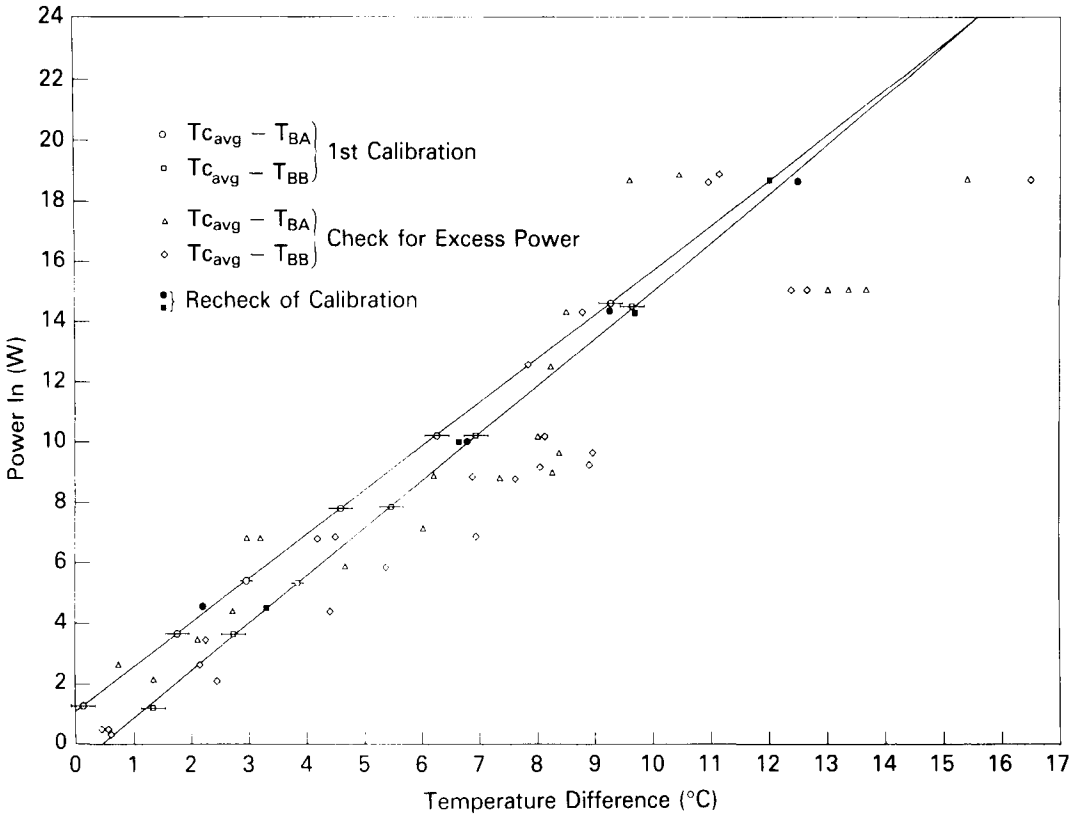

Fig. 2. Calibration curves for cell 4.

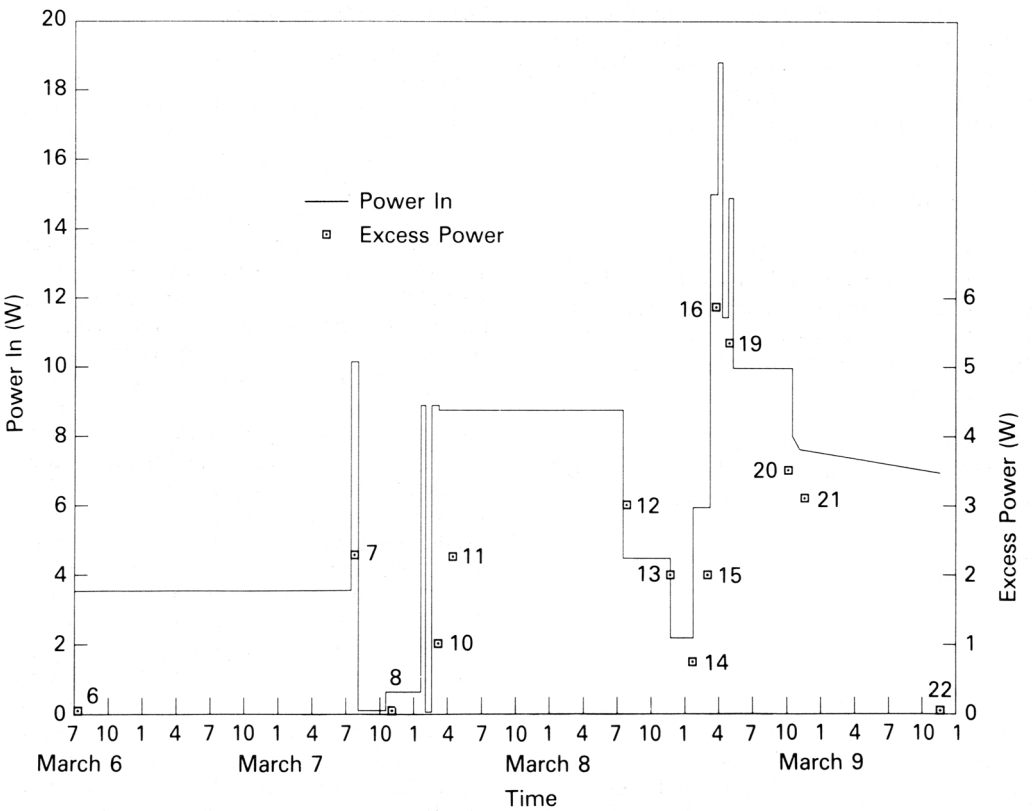

Fig. 3. Power versus time for cell 4.

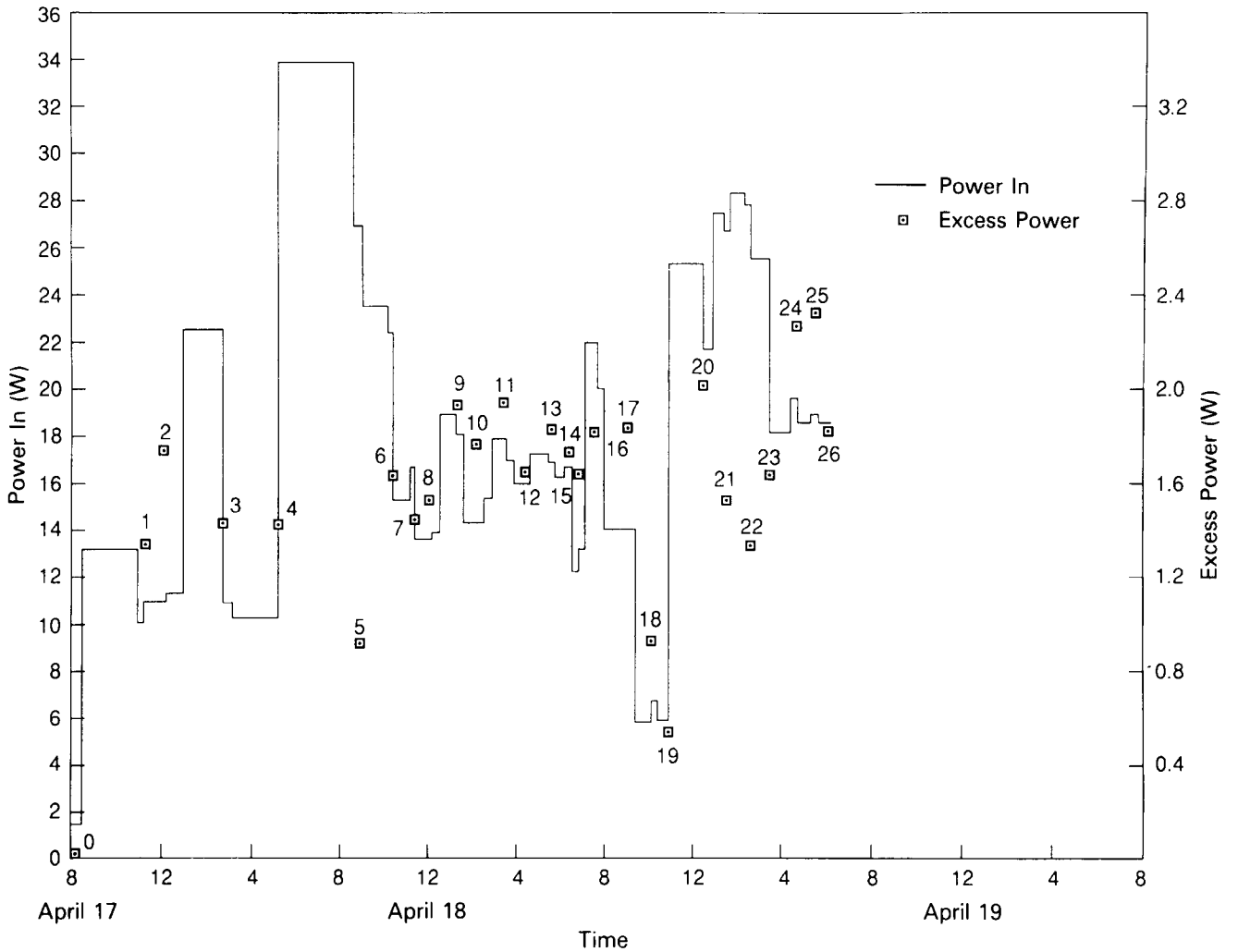

Fig. 4. Power versus time for cell 5.

TABLE I

Cell 4 Data

Data Point	I (A)	i (A/cm^2)	Voltage (V)	Temperatures (°C)						P (W)	P_{ex} (W)
				T_{CA}	T_{CB}	T_{BA}	T_{BB}	δT_a	δT_b		
10	0.941	0.235	9.560	26.3	26.4	20.2	19.5	6.15	6.85	9.00	1.2, 1.3
11	1.009	0.252	8.791	26.9	26.9	19.6	19.3	7.3	7.6	8.87	3.0, 2.6
12	1.060	0.265	8.815	28.3	28.3	20.3	20.3	8.0	8.0	9.34	3.6, 2.8
13	0.641	0.160	6.893	23.0	23.2	---	18.7	2.7	4.4	4.42	---, 1.9
14	0.383	0.096	5.590	20.3	20.5	19.2	18.1	1.2	2.3	2.14	0.6, 0.8
15	0.780	0.195	7.633	24.1	24.2	19.5	18.8	4.65	5.35	5.98	2.0, 2.0
16	1.700	0.425	11.115	36.3	36.7	21.2	20.1	15.3	16.4	18.89	5.0, 6.8
17	1.448	0.362	10.426	33.0	33.0	20.1	20.7	12.9	12.3	15.10	5.2, 4.0
18	1.47	0.367	10.425	33.5	33.6	20.2	20.9	13.4	12.65	15.32	5.7, 4.3
19	1.47	0.369	10.423	33.7	33.9	20.2	20.9	13.6	12.9	15.32	6.1, 4.7
20	1.092	0.273	9.021	29.6	29.2	21.1	20.5	8.3	8.9	9.85	3.6, 3.8
21	0.874	0.218	8.091	26.3	26.6	20.4	19.6	6.05	6.85	7.07	3.0, 3.2

TABLE II

Cell 5 Data

Data Point	I (A)	i (A/cm^2)	Voltage (V)	Temperatures (°C)						P (W)	P_{ex} (W)
				T_{CA}	T_{CB}	T_{BA}	T_{BB}	δT_a	δT_b		
1	0.881	0.22	10.736	34.6	35.5	22.8	23.9	12.25	11.15	9.46	1.35, 1.2
2	0.990	0.247	11.307	37.2	38.2	23.4	24.5	14.3	13.2	11.2	1.7, 1.5
3	0.954	0.238	11.10	37.0	37.8	24.1	24.9	13.3	12.5	10.6	1.6, 1.0
4	0.920	0.23	10.87	37.0	37.8	24.6	25.5	12.8	11.9	10.0	1.6, 1.1
5	1.915	0.479	14.00	56.5	57.5	27.8	29.3	29.2	27.7	26.8	0.9, 0.8
6	1.663	0.416	13.4	52.3	53.0	27.4	28.7	25.3	24.0	22.28	1.6, 1.3
7	1.322	0.331	12.3	45.4	46.1	26.7	27.8	19.1	18.0	16.26	1.5, 1.3
8	1.167	0.292	11.7	42.5	43.2	26.3	27.3	16.6	15.6	13.65	1.7, 1.4
9	1.401	0.35	12.6	47.6	48.4	27.2	28.0	20.8	20.0	17.65	2.2, 1.6
10	1.23	0.307	12.1	44.3	45.0	26.6	27.7	18.05	16.95	14.88	1.9, 1.6
11	1.34	0.335	12.5	46.5	47.4	26.9	28.0	20.1	19.0	16.75	2.1, 1.8
12	1.282	0.321	12.53	45.5	46.2	26.7	27.8	19.15	18.05	16.06	1.8, 1.5
13	1.326	0.332	12.6	46.5	47.2	27.1	27.9	19.75	18.95	16.7	2.15, 1.5
14	1.294	0.323	12.5	45.9	46.6	27.0	28.0	19.25	18.25	16.18	1.95, 1.5
15	1.088	0.272	11.7	41.6	42.4	26.3	27.3	15.7	14.7	12.73	1.8, 1.45
16	1.477	0.369	13.3	50.0	50.6	27.4	28.5	22.9	21.8	19.64	2.1, 1.6
17	1.191	0.298	12.3	44.1	44.8	26.6	27.6	17.85	16.85	14.65	2.1, 1.6
18	0.663	0.166	9.5	33.2	33.8	25.1	25.8	8.4	7.7	6.30	1.1, 0.7
19	0.604	0.151	9.1	32.3	32.5	25.4	25.5	7.0	6.9	5.5	1.0, 0.0
20	1.54	0.385	13.8	52.6	52.8	28.4	28.8	24.3	23.9	21.25	2.6, 1.4
21	1.80	0.450	14.7	58.2	58.6	29.2	30.0	29.2	28.4	26.46	1.9, 1.1
22	1.854	0.464	15.0	59.9	60.1	29.5	30.5	30.5	29.5	27.8	1.7, 1.0
23	1.719	0.430	14.8	57.6	57.9	29.5	30.2	28.2	27.6	25.4	2.0, 1.0
24	1.408	0.352	13.8	51.4	51.8	28.8	29.4	22.8	22.2	19.4	2.7, 1.8
25	1.363	0.341	13.65	50.6	50.9	28.6	29.4	22.2	21.4	18.6	2.7, 2.0
26	1.319	0.330	13.8	49.6	50.0	28.5	29.3	21.3	20.5	18.2	2.2, 1.5

TABLE III

Excess Heat Production

	Cell	
	4	5
Period of excess heat production (s)	1.73×10^5	1.22×10^5
Excess heat, Q (MJ)	0.35	0.2
Average excess power, P_{avg} (W)	2.0	1.6
Electrode area (cm^2)	4	4
Average areal specific excess power (W/cm^2)	0.5	0.4
Electrode volume (cm^3)	0.4	0.4
Average specific excess power (W/cm^3)	5	4

Excess Power as a Function of Current Density

The TRM predicts three significant features for the case in which excess power is explored as a function of current density with the electrolyte temperature held constant[1]:

1. There are linear regions where, to a good approximation, the excess power increases directly with the current density.

2. Between two neighboring linear regions, there is a transition region in which the excess power versus current density curve for the lower current density linear region has its slope decreased to give a relative peak excess power followed by a relative minimum of excess power associated with a "cusp" in the excess power curve. The next linear region begins to the right of the cusp.

3. The TRM predicts that at a high enough current density, the excess power versus current density curve will "roll over" to zero.

Figure 5, a duplicate of Fig. 13 of Ref. 1, displays these features. (Reference 1 shows how the mathematics of the TRM produces these features and provides a physical explanation for them.) Least-squares fits of the TRM to the experimental data of cells 4 and 5 are shown, respectively, in Figs. 6 and 5. All three features predicted by the TRM are seen for the case of cell 5 (Fig. 5). (Note, however, as indicated in Ref. 1, that the data of cell 5 for this "constant temperature" experiment is associated with two temperatures. Thus, the data points associated with a current density below 330 mA/cm^2

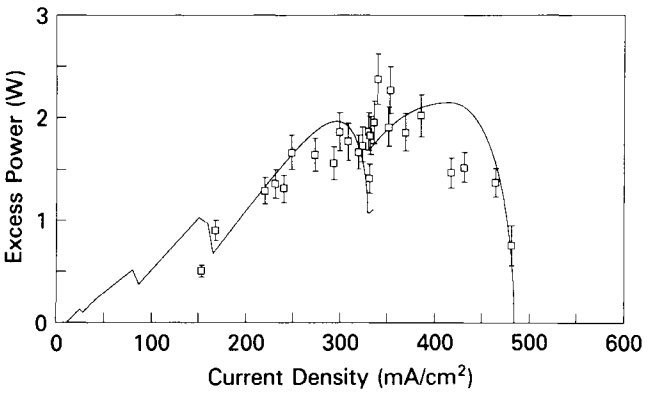

Fig. 5. Excess power versus current density (temperature held relatively fixed) based on the data from cell 5 showing actual data points (error bars) and the curve (solid line) generated by the TRM.

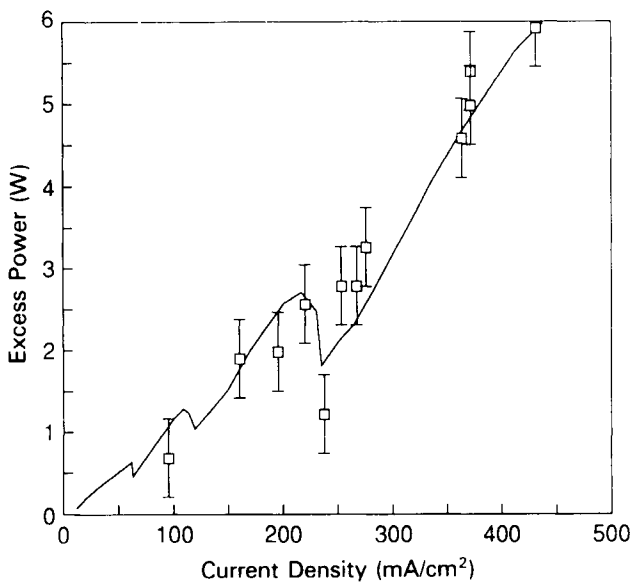

Fig. 6. Cell 4 data showing the fit of the TRM. The solid curve is generated using the TRM. The low-lying data point at 230 mA/cm^2 is now seen to be located at a cusp predicted by the TRM. The fit is not much better than that in Fig. 7, so that this constitutes only skimpy evidence in support of the TRM.

are associated with an average temperature of 312 K, while those above that current density are associated with an average temperature of 329 K. Thus, as Ref. 1 explains, the two groups of data were fit with the TRM using these two temperatures. Figure 5 thus displays the two theoretical segments "stitched" together.) Approximately 30 min elapsed between the taking of successive data points to achieve a steady state.

The cell 4 data (Figs. 6 and 7) were taken after Bush had arrived at the form of his model presented in Ref. 1, but before some of its interesting consequences were apparent. Nothing at that time suggested that there was anything special about the low-lying data point shown in Fig. 7 at a current density of ~230 mA/cm^2. In fact, it was thought that the large deviation of this data point from the straight line shown in Fig. 7 indicated that a steady state had not been

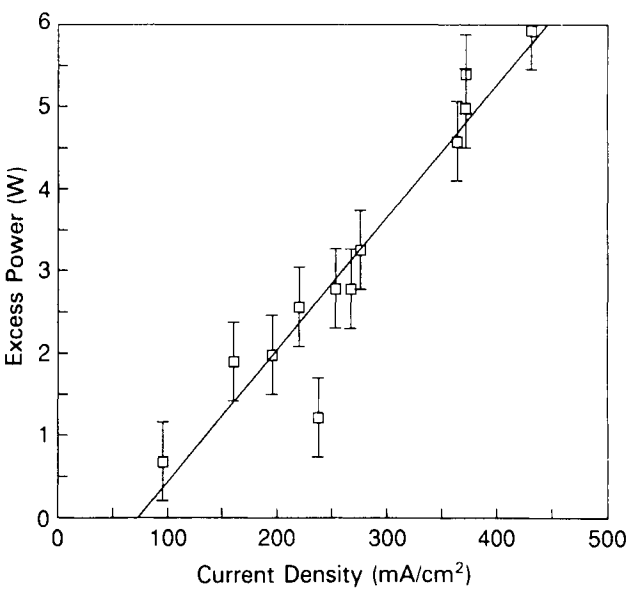

Fig. 7. Plot of excess power versus current density for cell 4 with cell temperature held relatively fixed.

reached in the case of that data point. Bush then realized that the present form of the TRM with the important energy shift would lead to the prediction of relative minima (cusps) in a plot of excess power versus current density with the temperature held constant. Figure 6 shows the fit of the TRM as a solid curve with a cusp (relative minimum) at ~230 mA/cm^2. However, the data point at this current density was the only feature in the cell 4 data that gave any indication of the possible correctness of the model. It was later found that the model gave a good fit to the data of cell 5. In the experiment with cell 5, the TRM was, in fact, employed to suggest where data points should be taken in order to check the model.

In the case of cell 4, it is conjectured that the current density was not large enough to cause a rollover to zero of the excess power at the upper end. As discussed in Ref. 1, the difference in the energy shift (which may be associated with overpotential) in cells 4 and 5 could account for a higher threshold current density in the case of cell 4 being necessary to achieve rollover to zero excess power.

Excess Power as a Function of Temperature

In this experiment, the electrode current density was held constant at 252 mA/cm^2, and the excess power was monitored as a function of cell temperature. Table IV lists the data for this experiment, while Fig. 8, taken from Fig. 18 of Ref. 1, indicates the good fit of the model to the data. Bush[1] discussed why this cooling would be effective in boosting the excess heat output in the context of the TRM.

CONCLUSION

Figures 5 and 8, based on Figs. 13 and 18, respectively, of Ref. 1, show the good fit of the TRM to the data in two radically different types of experiments. We conclude, in agreement with Ref. 1, that not only does this provide strong support for the TRM, but it also strengthens the claim that the Fleischmann-Pons excess heat effect is genuine.

TABLE IV

Cell 5 Data for Constant Current*

Point	Temperature (K)			P_{ex} (W)
	T_{CA}	T_{CB}	T_{avg}	
1	331.2	331.6	331.4	0
2	326.9	327.7	327.3	1.45
3	323.5	324.0	323.8	1.15
4	321.1	321.4	321.2	2.0
5	319.0	319.5	319.2	2.2
6	317.4	318.0	317.7	1.9
7	316.3	316.8	316.6	1.65
8	314.8	315.5	315.2	2.5
9	313.4	313.7	313.6	2.45
10	312.0	312.8	312.4	2.83
11	310.7	311.3	311.0	2.5
12	309.7	310.1	309.9	2.2

*Current = (1.012 ± 0.002) A, cathode surface area = (4 ± 0.2) cm^2, and current density = (0.252 ± 0.13) A/cm^2.

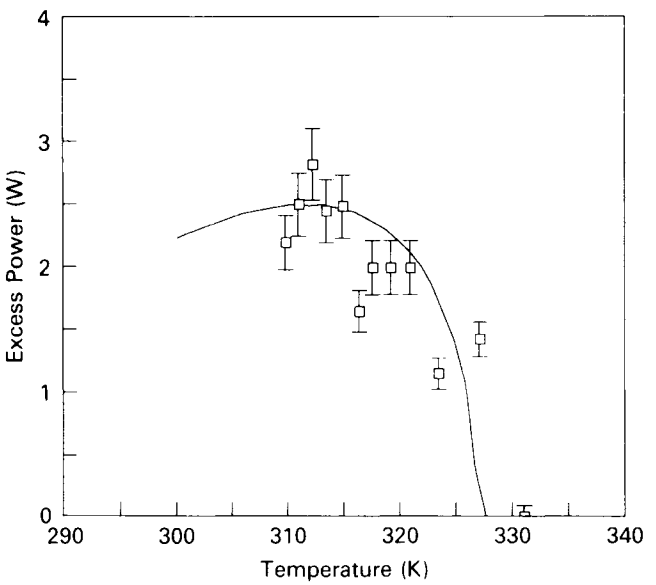

Fig. 8. Excess power versus temperature at constant current density for cell 5. The good fit of the TRM (solid line) to the data points (errors bars) in this "cooling" experiment lends strong support to the TRM.

We recently worked with a new cell design that we feel is superior from the standpoint of the calorimetry. We have also added a computerized data acquisition system that has immensely improved the gathering and processing of calorimetric data. Two new cells were run as regular (light) water blanks but gave no evidence of excess power or heat. However, we have again obtained data that exhibit the interesting "fine structure": "hills" separated by a "V-shaped" valley with a cusp at the bottom in a plot of excess heat versus current density (as in Fig. 5), which is fit by the TRM. Storms[3] has suggested that, since our equipment is so radically different from that employed for the data of this paper, it is, assuming the data's correctness, essentially as if an independent corroboration of our experimental work, as well as the predictions of the TRM, had been carried out.

ACKNOWLEDGMENTS

It is a pleasure to thank Steven Crouch-Baker (University of California–Los Angeles) and Howard Rogers (Hughes) for their suggestions and help in providing a recombiner. We wish to thank George Miley, editor of *Fusion Technology*, and three anonymous referees for suggestions to improve the original manuscript. We are grateful to the following California State Polytechnic University (Cal Poly) undergraduates for their assistance: Roger Smith, Sean Smith, and Adam Phipps. The support and encouragement of the following individuals within the College of Science at Cal Poly is greatly appreciated: Ray Shiflett (former dean), David Moriarty (dean), Victor Abegg (associate dean), and Harvey Leff (chairman of the physics department). Raymond Fleck (director of research, Cal Poly) is thanked for his help and enthusiasm. Johnson-Matthey and its representative, David Thompson, are gratefully acknowledged for a metals loan. Phillip Armstrong and Ron Ellis of Los Alamos National Laboratory are thanked for metal fabrication. Finally, we wish to express our profound gratitude to Southern California Edison Company (research representative: N. J. Kertamus) and to Wind River Resources (president: J. Ignat) for their financial support and encouragement.

REFERENCES

1. R. BUSH, "Cold 'Fusion': The Transmission Resonance Model Fits Data on Excess Heat, Predicts Optimal Trigger Points, and Suggests Nuclear Reaction Scenarios," *Fusion Technol.*, **19**, 313 (1991).

2. M. FLEISCHMANN and S. PONS, "Electrochemically Induced Nuclear Fusion of Deuterium," *J. Electroanal. Chem.*, **261**, 301 (1989).

3. E. STORMS, Los Alamos National Laboratory, Private Communication (Feb. 1991).